J. Synchrotron Rad. (1998). **5**, 896–898

Surface X-ray scattering system at the SRRC

Chia-Hung Hsu* and Mau-Tsu Tang

Synchrotron Radiation Research Centre, Hsinchu 30077, Taiwan. E-mail: chsu@alpha1.srrc.gov.tw

(*Received 4 August 1997; accepted 16 October 1997*)

A UHV surface X-ray scattering system has been constructed at the SRRC, providing users with a state-of-the-art system for performing X-ray scattering studies of two-dimensional crystallography, *in situ* growth mechanisms as well as phase transitions of surfaces and interfaces. A study of the phase transition of the Si(001) reconstructed surface was conducted to commission both the scattering system and the SRRC X-ray beamline. The detailed design and performance of the SRRC surface X-ray scattering system together with the results of the Si(001) study are presented.

Keywords: surface X-ray scattering; diffractometers.

1. Introduction

Studies of two-dimensional structure in the near-surface and interface regime have attracted wide interests both from scientific and technological points of view. X-ray scattering has proven to be a powerful tool for surface-related studies. X-rays are scattered weakly by materials as compared with electrons and other charged particles. Consequently, the multiple scattering effects, which are important in electron scattering, are negligible in X-ray scattering and most of the experimental results can be interpreted by simple kinematical theory. The weak interaction of X-rays with materials also reflects their deep penetration into the samples and renders X-ray scattering an excellent tool to probe the buried interface non-destructively. Besides, X-ray scattering is a technique with high spatial resolution and long coherent length, ideal for measuring systems with long-region ordering to tens of thousands of ångströms.

Nevertheless, X-ray scattering is inherently insensitive to the relatively small amount of atoms in the surface or interface region. Surface X-ray scattering was not practical until the recent advances both in experimental techniques and in X-ray light sources. Grazing-incidence scattering geometry exploits the total external reflection effect and confines X-rays to the region of less than 50 Å from the surface. It greatly enhances surface sensitivity and also eliminates the background from bulk scattering. The advent of bright and highly collimated synchrotron radiation increases the signal-to-noise ratio of surface-scattering signals to a satisfactory level. Moreover, energy tunability of synchrotron radiation makes it possible to combine anomalous scattering with surface scattering techniques to obtain additional information. Since then, a wide range of problems, such as surface morphology, two-dimensional crystallography, surface phase transitions, and the growth mechanism of thin films, have already been studied using surface X-ray scattering (Robinson, 1993, and references therein). Recently, the development of third-generation synchrotron radiation facilities has made it possible to probe the surface collective excitation by surface inelastic X-ray scattering and opened up a new era in surface science research.

To ensure the success of surface-scattering measurements, the experimental set-up has to fulfil the following four basic requirements: (i) a UHV environment allowing the sample to last for as long as the experiment execution, (ii) a diffractometer to provide the degrees of freedom for sample and detector to match the diffraction condition, (iii) complimentary surface diagnostic tools for sample preparation and preliminary characterization, and (iv) computer software for goniometer control and data acquisition. The development of surface X-ray scattering apparatus has evolved from the simple portable cell to very sophisticated UHV scattering systems. In this article we will describe the UHV surface X-ray scattering system recently built at the SRRC, which allows us to conduct various *in situ* studies of thin-film growth and surface phase transitions.

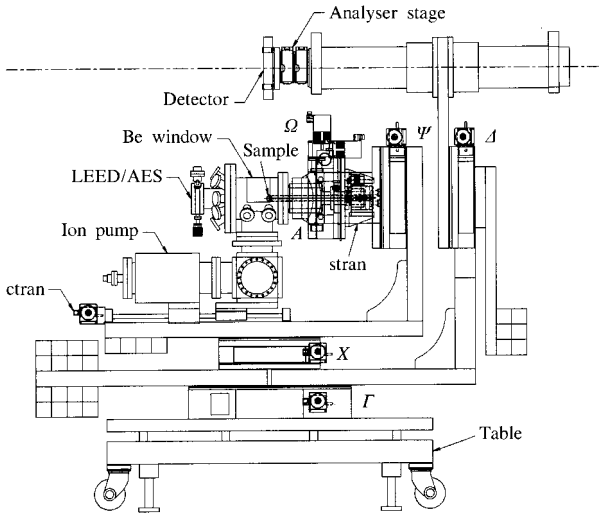

Figure 1
The layout of the UHV surface X-ray scattering system at the SRRC. The rotation axes, as well as major components of equipment, are marked.

2. Instrumentation design

The SRRC surface X-ray scattering system is part of the wiggler X-ray beamline end-station set-up and is the only surface X-ray scattering facility in Taiwan. It is expected that this facility will be used for various kinds of surface studies and by many users. Therefore, being simple and flexible are our design goals, besides the two fundamental requirements of high momentum resolution and large reciprocal space coverage. Considering these factors, the scattering system appears as shown in Fig. 1. The entire system is composed of a diffractometer, movable table, vacuum system and diagnostic/preparatory instruments. The widely used software *SPEC* is employed for system control and data acquisition. The scattering geometry and the design of each hardware component are described in detail in the following sections.

2.1. *Scattering geometry*

The application and performance of a diffractometer are ultimately determined by the scattering geometry it is based on. Our design adopted the '2 + 2' z-axis type of scattering geometry (Evans-Lutterodt & Tang, 1995) as the framework, where both detector and sample have two degrees of freedom. With this geometry, the motion of the sample is not constrained by the

vacuum chamber and thus a large incident angle can be readily reached. Moreover, the detector has a full range of in-plane and out-of-plane movements. These features result in optimal access to reciprocal space. However, the performance of this type of diffractometer strongly depends on the accuracy in sample alignment. The lack of a mechanism to fine-tune the sample orientation after the initial sample mounting is the disadvantage of this geometry. This becomes particularly troublesome when the sample undergoes treatment over a large temperature range and may move after initial alignment. To overcome this problem, we added two additional degrees of freedom to the sample. These two degrees of freedom, implemented by a rotation stage and a Eulerian cradle, allow either the sample surface normal or a particular reciprocal lattice vector to be aligned precisely with the azimuthal axis of the diffractometer. Consequently, one can apply definite incident- or exiting-angle scattering modes unambiguously according to specific experiment requirements. This six-circle design combines the advantages of both four-circle (Fuoss & Robinson, 1984) and z-axis (Brennan & Eisenberger, 1984) types of scattering geometry.

2.2. *Diffractometer and heavy-duty XY table*

The diffractometer possesses ten different movements and all are driven by stepping motors. The assignment of each degree of freedom is marked in Fig. 1. The sample is mounted onto an assembly of three goniometers, Ω, A and Ψ, resembling the combination of φ, χ and θ circles of conventional four-circle diffractometers, except that the χ circle is replaced by a pair of arcs A in the current design. This assembly is then carried by a vertical-axis circle X. Ω and A are used to align a particular vector, *e.g.* surface normal or a crystallographic axis, of the sample to the Ψ axis. The function of X and Ψ is to rotate the desired reciprocal vector $\mathbf{G}$ to the position where the detector intercepts. The detector is mounted onto a horizontal-axis circle Δ, which sits on another vertical-axis circle Γ. In terms of function, our diffractometer is equivalent to the six-circle diffractometers built by Ferrer & Comin (1995) and Takahasi *et al.* (1996). However, in our design the detector is carried by two orthogonal circles and moves on a spherical surface centred on the sample, in contrast to the aforementioned six-circle systems where the detector out-of-plane motion is achieved by delicately coupling a linear translation with a rotation. Therefore, our design is technically easier to implement and inherently more accurate. Moreover, the detector remains at a constant distance from the sample so that no additional corrections are required to compensate the varying sample–detector distance and detector acception angle.

In addition to a Huber 414 two-circle goniometer mounted on the detector arm as an analyser stage, the diffractometer has another two linear degrees of freedom: sample translation (stran) and chamber translation (ctran). stran translates the sample in and out of the vacuum chamber along the Ψ axis. This motorized mechanism has a resolution better than 10 µm. It facilitates accurate and quick positioning of the sample at the diffractometer centre and significantly eases the sample alignment process. ctran is a slide mounted on top of the X circle. It moves the entire vacuum system relative to the sample along the Ψ axis. This allows the sample to be placed at the diagnostic or scattering positions, which are 3.5" apart, without actually moving the sample, and thus ensures sample alignment.

To facilitate accurate and quick diffractometer alignment, the entire diffractometer, together with the vacuum system, are carried by a high-precision XY movable table. The table has four degrees of freedom: one horizontal and three vertical translations. With various combinations it provides two transverse linear motions as well as roll and pitch rotational motions. With the diffractometer and vacuum system (weighing about 3 tons) on the table, each motion has an accuracy of better than 100 µm.

2.3. *UHV system*

Considering the goal of having high flexibility to match various experimental requirements, we adopted the idea of modular implementation in designing the UHV system. With modular implementation, different requirements can be readily satisfied by replacing one or two modules, such as the 12" diagnostic flange, sample manipulator or even the scattering chamber. The whole system can be divided into the following modules: scattering chamber, 12" diagnostic flange, sample manipulator, bottom chamber, and pumping system. Some of the modules are described in the following.

The scattering chamber is a T-shaped vacuum chamber with a diameter of 8" and a length of 10.23". A piece of Be is electron-beam-welded to the chamber to form the X-ray window. The Be window is 4.5" wide and covers an angle of 200°. The 4.5" width allows both the incident and exit angles to be larger than 45° so that it is possible to explore experiments involving polarization effects. The Be used is PF-6 graded containing less than 700 p.p.m. iron impurity. The 0.02"-thick window results in a transmission of 70% at 8 keV. The ends of the scattering chamber are 12" and 10" conflat flanges, which are connected to the diagnostic flange and the rotary seal-bellows assembly, respectively. A short segment of form bellows is incorporated between each end flange and the body of the scattering chamber to isolate the Be window from the bending stress introduced by the end flanges. In addition to an 8" flange to connect to the bottom chamber, there are four 2.75" and two 1.333" flanges which are used to mount equipment such as vacuum gauge, residue gas analyser and quartz thickness monitor.

The scattering chamber is coupled to the diffractometer *via* a differentially pumped rotary seal-bellows assembly. We used a commercial Thermionics RNN-250 rotary seal and a welded bellows with a stroke of over 10". The 4.25" inner diameter of the bellows limits the largest reachable angle of arcs A to be $\pm 10°$ before the 1"-diameter sample manipulator rod touches its inner wall. This assembly is connected to the diffractometer through a specially designed double-sided flange. The other side of the double-sided flange is connected to the sample translation mechanism, stran, which in turn is joined to the sample manipulator. A 12" diagnostic flange is mounted on the other end of the scattering chamber. It is a cluster flange with one 6" and eight 2.75" conflat flanges. The 6" flange is used to accommodate LEED/AES optics or load-lock systems. The 2.75" flanges are divided into two sets focusing on the scattering position and diagnostic position. Equipment, such as the electron-beam evaporator and IR pyrometer, is mounted on the former set so that an *in situ* study during surface growth or temperature-induced phase transition can be conducted. Equipment, such as an ion sputtering gun, is mounted on the latter set for use, together with LEED/AES, for sample cleaning and diagnostics.

The system is equipped with a $340\,l\,s^{-1}$ ion pump, a Ti sublimation pump with a cryogenic shroud and a $250\,l\,s^{-1}$ turbomolecular pump. The whole vacuum system becomes stand-alone when the gate valve to the turbomolecular pump is closed.

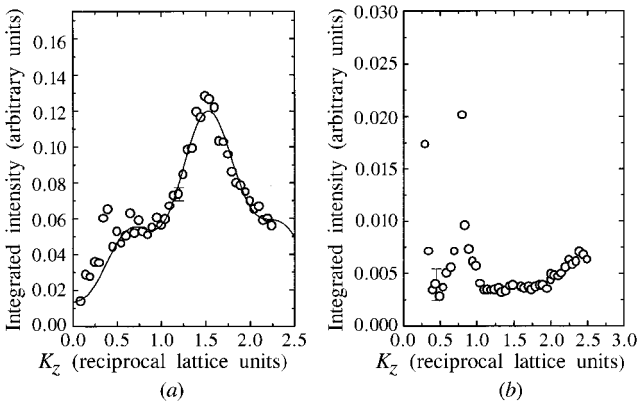

Figure 2
(*a*) Scattering intensity *versus* vertical momentum transfer K_z of Si(001) (2 × 1) half-order reconstruction rod (3/2 1) measured at room temperature. (*b*) Scattering intensity *versus* vertical momentum transfer K_z of the Si(001) c(4 × 2) quarter-order reconstruction rod (5/4 1/2) measured below 150 K.

2.4. *Diagnostic/preparatory instruments*

Depending on individual experimental requirements, various surface diagnostic/preparatory equipment can be mounted on the diagnostic flange or the scattering chamber. Currently, we have an electron-beam evaporator, ion sputtering gun, IR pyrometer, RGA and quartz thin-film thickness monitor for sample preparation, as well as a rear-view LEED system and retarded field AES for sample characterization. This apparatus is sufficient to perform most surface studies.

3. Experimental results

For the purpose of machine commissioning, we conducted a measurement on the reconstructed Si(001) surface at room temperature and at 150 K in December 1996. The experiment was performed at the SRRC wiggler X-ray beamline using an incident photon energy of 8.8 keV. A Si(001) wafer, 2" × 1" in size, was pretreated chemically following the standard RCA method to form a stable Shiraki oxide film. The sample was subsequently mounted into the UHV chamber, which was pumped down to 10^{-10} torr. The sample was flashed several times up to 1100 K followed by thermal annealing by resistive heating; a well ordered (2 × 1) reconstruction pattern was observed by LEED.

Surface X-ray scattering was then performed to measure the (1 1) crystal truncation rod as well as three half-order reconstruction rods, (1/2 0), (3/2 0) and (3/2 1). Shown in Fig. 2(*a*) is the scattering intensity *versus* vertical momentum transfer K_z of the (3/2 1) rod. The modulation of rod intensity indicates a relaxation structure along the surface normal. The sample was then cooled to 150 K by introducing liquid nitrogen into the sample manipulator. Limited by beam time, only one quarter-order rod resulting from the c(4 × 2) reconstruction surface was measured, as displayed in Fig. 2(*b*). A linear detector was employed in all the measurements. With the current experimental set-up, the largest horizontal scattering angle is about 70°, limited by the beam-pipe support. In the preliminary data analysis, eight non-equivalent in-plane half-order peaks were used to generate a surface Patterson map. The surface projection of the dimer bond length is determined to be 2.41 Å. This bond length was in turn used as a parameter in a four-layer relaxation model to fit the three half-order rods. The tilted angle of the dimers determined from the best fit, depicted by the solid curve in Fig. 2(*a*), was about 12.6°, which is less than other measurements (Felici *et al.*, 1997; Jayaram *et al.*, 1993). The detailed data analysis is still in progress.

4. Conclusions

We have designed and constructed a versatile UHV surface X-ray scattering system at the SRRC. The performances of both the hardware and software set-ups are satisfactory. In particular, our design drastically reduced the time for diffractometer and sample alignment to within a few hours and all the operations are much easier and more accurate. With this system, exciting results for surface structure determination, surface growth mechanisms and surface phase transitions are expected.

The authors express their thanks to Dr K. Evans-Lutterodt for very helpful discussions on the conceptual design, and to Mr L. Wenzel for an excellent job in the detail design. The authors acknowledge the technical support provided by SRRC personnel, particularly, Mr J.-Y. Liu and Mr J.-M. Chuang.

References

Brennan, S. & Eisenberger, P. (1984). *Nucl. Instrum. Methods*, **222**, 164–167.
Evans-Lutterodt, K. W. & Tang, M.-T. (1995). *J. Appl. Cryst.* **28**, 318–326.
Felici, R., Robinson, I. K., Ottaviani, C., Imperatori, P., Eng, P. & Perfetti, P. (1997). *Surf. Sci.* **375**, 55–62.
Ferrer, S. & Comin, F. (1995). *Rev. Sci. Instrum.* **66**, 1674–1676.
Fuoss, P. H. & Robinson, I. K. (1984). *Nucl. Instrum. Methods*, **222**, 171–176.
Jayaram, G., Xu, P. & Marks, L. D. (1993). *Phys. Rev. Lett.* **71**, 3489–3492.
Robinson, I. K. (1993). *Handbook on Synchrotron Radiation*, Vol. 3, edited by G. S. Brown & D. E. Moncton, pp. 221–266. Amsterdam: North-Holland.
Takahasi, M., Nakatani, S., Ito, Y., Takahasi, T., Zhang, X. W. & Ando, M. (1996). *Surf. Sci.* **357/358**, 78–81.